# Covariance for time series on Lie groups applied to climbing motion analysis

Jeremie BOULANGER[1], Ludovic SEIFERT[2], Dominic ORTH[3]

[1]Laboratoire CRISTAL, Equipe SIGMA, Lille (France) ,

[2]Laboratoire CETAPS, Rouen (France),

[3]Faculty of Behavioral and Movement Sciences, Vrije Universiteit, Amsterdam, (The Netherlands)

jeremie.boulanger@univ-lille1.fr

**Résumé –** Cet article présente une méthode pour calculer une matrice de covariance entre deux signaux à valeur sur $SO(3)$. Pour chacun, sa moyenne est calculée. Après avoir projeté chaque signal dans le plan tangent de sa moyenne via l'application $\log$, chaque projection est translatée pour être dans le même plan tangent. Une matrice de covariance classique peut alors être calculée. Cette mesure peut alors être utilisée pour l'étude du mouvement humain. Par exemple, en attachant des capteurs inertiels au cou et au bassin d'un grimpeur, il est possible d'estimer la coordination du roulis de différentes parties de son corps, indicateur de performance du grimpeur.

**Abstract –** This article describe a method to measure a covariance matrix between two $SO(3)$ based signals. For each one, the mean value is computed. After applying the $\log$ map to project each signal in the tangent space of its mean, they are both translated to the same tangent space. A classic covariance matrix can then be determined. Using IMUs (Inertial Measurement Unit) attached to the hip and the neck of an indoor climber, it can be used to create an indicator of body kinematics coordination. Studying such coordinations might be useful for determining the climber skills.

## 1 Introduction

Indoor climbing requires specific motor skills and coordination due to quadrupedal locomotion on a vertical plain using only limb extremities such as fingers and toes. Analyzing the rolling motion of the body is a good way to indicate the ability of the climber to control and to exploit the gravitational forces. For example, given the choice, beginners tend to climb with the body face to the wall, leading to the emergence of a horizontal hold grasping pattern, like "climbing a ladder".

Conversely, expert climbers use rolling motion of the trunk, leading the emergence of alternating positions such as with the body face on, side on or obliquely positioned relative to the wall, somewhat like "opening/closing a door" [2]. This was assumed to be a more skilled behavior, reflecting adaptation of the body's orientation to the wall, supporting fluent climbing performance [1]. It was hypothesized that practicing during a learning protocol where the route is design to alternate those two behaviors can help beginners to learn side to the wall body position.

Once an individual has learned these two behaviors, an individual could both exploit the pre-existing behavioral repertoire (i.e., trunk face to the wall) and use the newly learned behavior (i.e., rolling motion of the trunk side or obliquely to the wall), which can finally be observed by (i) greater rolling motion of trunk and (ii) greater variability of rolling motion of trunk through a time-series. Such indicators have already been measured in [2] for example.

However, it is also assumed that rolling motion of the trunk could be achieved by rolling only the hip, only the shoulders, simultaneously hips and shoulders but in opposite sides or simultaneously hips and shoulders but in the same direction. This leads to a comparison between the orientation of the hips and the orientation of the shoulders with respect to the climbing wall. For each climb, IMUs attached to the hips and the shoulders records data [3] which leads to the orientation of each IMU. These orientations are $SO(3)$ valued signals. Mathematically speaking, it corresponds to finding a way to measure the covariance between two $SO(3)$ based signals.

The reference frame is the one obtained by placing a sensor against the wall aligned vertically. For example, if the hip orientation is $I_3$, then the hips should be facing the wall.

## 2 Method

Despite that the results presented here are dedicated to $SO(3)$, they can be easily generalized for any Lie group.

## 2.1 Geometry of $SO(3)$

The Lie group used in this case is the special orthogonal group of $\mathbb{R}^3$ :

$$SO(3) = \{R \in \mathbb{R}^3 | RR^T = I, \det(R) = 1\}.$$

The Lie algebra associated to $SO(3)$ is the set of skew symmetric matrix :

$$\mathfrak{so}(3) = \{r \in \mathbb{R}^3 | r^T = -r\}.$$

Let $\phi : \mathbb{R}^3 \to \mathfrak{so}(3)$ be the bijection :

$$\phi \begin{pmatrix} r_0 \\ r_1 \\ r_2 \end{pmatrix} = \begin{pmatrix} 0 & -r_2 & r_1 \\ r_2 & 0 & -r_0 \\ -r_1 & r_0 & 0 \end{pmatrix}. \quad (1)$$

The algebra $\mathfrak{so}(3)$ is the tangent space to $SO(3)$ at the point $I$. The tangent space at the point $R \in SO(3)$ is denoted $T_R SO(3)$.

The $\exp$ and $\log$ maps are the usual matrix exponential and its inverse. The $\exp$ map applied from $T_R SO(3)$ is denoted $\exp_R(.) = \exp(.)R$ and the $\log$ map applied from $R \in SO(3)$ is denoted $\log_R(.) = \log(.R^T)$. It shall be noted that the translation is here done by multiplying to the right. This is required as sensors might be mis-aligned (cf Section 2.3).

The geodesic distance $d : SO(3)^2 \to R^+$ is defined as :

$$d(R_1, R_2) = ||\phi^{-1}(\log(R_2^{-1}R_1)||_2.$$

## 2.2 Computing the mean

For Euclidean space based signals, centering the signals is needed for computing the covariance. Here, a similar step is realized. However, due to the geometry of $SO(3)$, an intrinsic mean is computed. Let $X_t \in SO(3)$ be a time series for $t \in [0, T]$ running on $SO(3)$ and let $\bar{X}$ be the mean of $\{X_t\}_{t\in[0,T]}$.

Computing the mean can be done via different algorithms. Here, two methods are presented, based on the definition of the mean [4], minimizing the function $\psi$ :

$$\bar{X} = \text{argmin}_Y \left\{ \psi(Y) = \int_{t\in[0,T]} d(Y, X_t)^2 dt \right\} \quad (2)$$

An important property is that for a fixed rotation $R \in SO(3)$, we have : $\overline{XR} = \bar{X}R$, similarly to classic Euclidean geometry [5].

### 2.2.1 Mean Shift

The usual method is the mean shift algorithm. It consists in an iterative algorithm whose minimization steps are preformed in a linear space [6]. Let $\bar{X}^k$ be a sequence defined by Algorithm 2.2.1.

**Algorithm 1** Mean shift algorithm

$\bar{X}^0 = X_{T/2}$
**for** Iteration $k = 1$ to $k_{max}$ **do**
  **for** $t = 0$ to $T$ **do**
    $x_t = \phi^{-1}\left(\log_{\bar{X}^k}(X_t)\right)$
  **end for**
  $\bar{x}^k = \frac{1}{T}\int_t x_t dt$
  $\bar{X}^k = \exp_{\bar{X}^{k-1}}(\phi(\bar{x}^k))$
**end for**

It can be proven that under proper conditions, the sequence $\left\{\bar{X}^k\right\}_k$ will converge to $\bar{X}$ from Equation 2. The number of iterations, here fixed to be $k_{max}$ can also be modified to stop the algorithm once the increments on $\bar{X}^k$ become small enough.

It should be noted that this method heavily requires the computation of $\log$. With a lot of samples, the computation, despite being linear, can be quite time consuming. This is needed to know the direction of the iteration to perform something similar to the gradient descent.

### 2.2.2 Simulated annealing

Instead of iterating to the proper direction to minimize equation 2, one could use a random step applied to several particles. With enough particles, compared to the dimension of the Lie group (in the case of $SO(3)$, the dimension is 3), the direction of the increment obtained from the mean shift algorithm will be visited [7, 8]. Considering $i_{max}$ particles, for $k_{max}$ iterations, the algorithm is presented in Algorithm 2.2.2.

**Algorithm 2** Simulated annealing algorithm

**for** Particle $P^i$ with $i = 0$ to $i_{max}$ **do**
  $P^i = X_{T/2}$
  **for** Iteration $k = 1$ to $k_{max}$ **do**
    • Candidate $C^i = \exp_{P^i}(\phi(c^i))$
    with $c^i \sim \mathcal{N}(0, I_3/\log(k+1))$
    • Accept $P^i = C^i$ with
    probability $\min\left(1, \psi(P^i)/\psi(C^i)\right)$
  **end for**
**end for**

Despite that this algorithm will require less computation of $\exp$ and $\log$, its output, the particles $P^i$ does not directly give the mean but a sampling from the distribution of the mean on $SO(3)$. An additional step will be required but for long time series $\{X_t\}$, the computation is being performed on a smaller set of data.

Another difference between these methods is that the mean shift only gives one value. If the time series is not stationary, it might completely bias the covariance in the next steps. The simulated annealing can be used in the case of piece-wise constant

mean.

### 2.3 Covariance

For two $SO(3)$ based time series $X_t$ and $Y_t$, we define :

$$\begin{aligned} x_t &= log_{\bar{X}}(X_t) \\ y_t &= log_{\bar{Y}}(Y_t) \end{aligned} \tag{3}$$

By rewriting $\log_{\bar{X}}(X_t) = \log(X_t\bar{X}^{-1})$, one can easily see the two steps performed via this operation :

— Centering : By multiplying by $\bar{X}^{-1}$, the data are translated around $I_3$. This is the equivalent of centering the data by translating the time series in classic covariance computation. The main interest now is that the time series $x_t$ and $y_t$ are now both in the same tangent space $T_I SO(3)$. They can therefore be compared.

— Linearization : The log operation realizes the linearization of the time series sample by sample. The linearization step should be performed for each sample with respect to the intrinsic mean contrary to an anti-development solution in order to prevent the creation of a drift due to a long term integration [9].

As $x_t$ and $y_t$ are both in $T_I SO(3) = \mathfrak{so}(3)$, $\phi^{-1}$ can be applied and the covariance is then defined as :

$$C(X,Y) = \text{cov}\left(\phi^{-1}(x_t), \phi^{-1}(y_t)\right) \tag{4}$$

where cov is the usual covariance in $\mathbb{R}^3$, $x_t$ is defined at Equation 3 and $\phi$ is defined at Equation 1.

It shall be noticed that in the case of a badly oriented sensor, the proper signal $X_t$ is recorded as $X_t R$, where $R$ is the rotation offset. By denoting $xr_t$ the linearization of $X_t R$ given by Equation 3, we have :

$$\begin{aligned} xr_t &= log_{\bar{X}R}(X_t R) \\ &= log_{\bar{X}R}(X_t R) \\ &= log_{\bar{X}R}(X_t R(\bar{X}R)^{-1}) \\ &= log_{\bar{X}R}(X_t \bar{X}^{-1}) \\ &= x_t. \end{aligned}$$

Therefore, a rotation offset does not affect the measure of the correlation.

## 3 Application

An application to a recorded signal is presented in Figure 2 for the sensor attached to the hips. Based on these linearized signals, a covariance matrix can be determined, based on Equation (4) :

| Hips ↓ Neck → | $Ox'$ | $Oy'$ | $Oz'$ |
|---|---|---|---|
| $Ox$ | 0.22 | 0.05 | −0.01 |
| $Oy$ | −0.04 | −0.01 | 0.02 |
| $Oz$ | 0.06 | 0.02 | −0.01 |

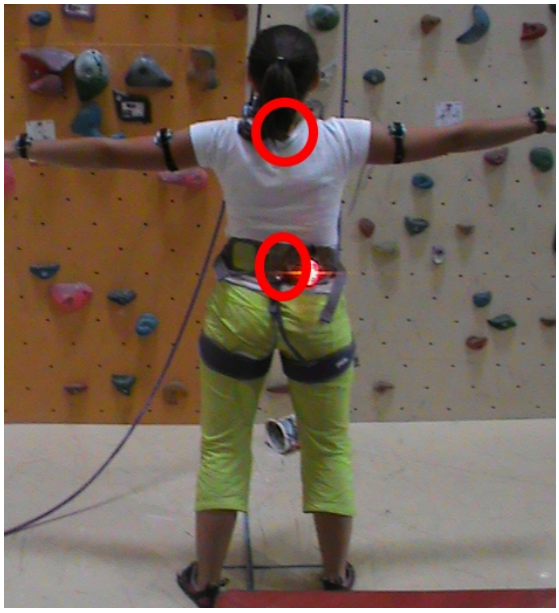

FIGURE 1 – Sensors attached to a climber. Only the ones circled in red are used in this article.

In this case, the highest covariance is around the $Ox$-axis (vertical) for the hips and the $Ox$ axis for the neck. This indicates that the hips and the shoulders are synchronized in their rolling motion. Even if not presented here, this method could also be used to determine the variance of each rotation signal, based on the variance definition from [2].

A short study based on one climber during a 17 sessions training program shows a large decrease in the diagonal terms of the covariance matrix, mainly for the component around the $Ox$ axis. For each sessions, three different climbing conditions were asked to the climber :

— Spontaneous climbing (no particular instructions)
— Climbing face to the wall
— Climbing side to the wall

| Session | Condition | $Ox/Ox'$ | $Oy/Oy'$ | $Oz/Oz'$ |
|---|---|---|---|---|
| 1 | Spontaneous | 0.20 | 0.06 | 0.06 |
| 1 | Face | 0.25 | 0.06 | 0.11 |
| 1 | Side | 0.31 | 0.08 | 0.11 |
| 17 | Spontaneous | 0.02 | 0.05 | 0.05 |
| 17 | Face | 0.03 | 0.05 | 0.06 |
| 17 | Side | 0.06 | 0.04 | 0.10 |

Results of the training sessions show a large decrease in the covariance terms. This seems to indicate that the climber tends to make uncorrelated shoulder and hip movements, offering him a larger range of possible motions, by releasing another degree of freedom.

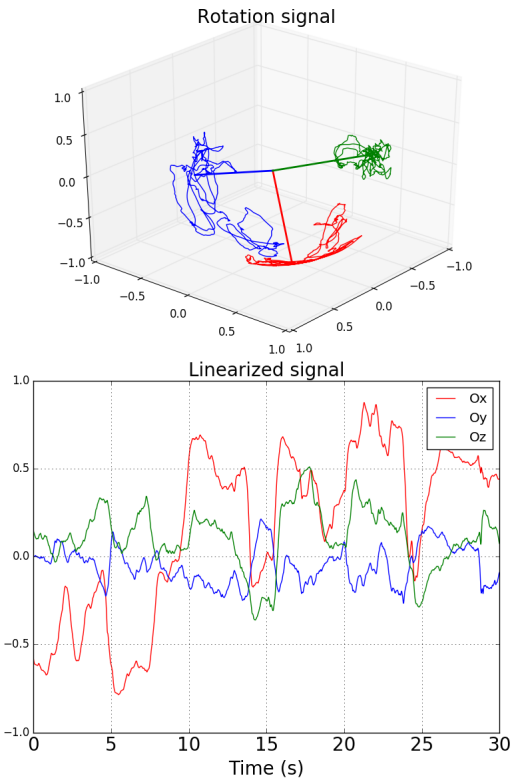


FIGURE 2 – (Top) : $SO(3)$ based signal sample is an orthonormal frame. Each color represents the evolution of each canonical vector. Final vectors are plotted. (Below) : Linearization of the top signal around its mean.

# 4 Limitations and openings

One limiting aspect to Equation 4 comes when the data is not stationary or when the data is not localized enough to be linearized. In the case when the data drives away from the intrinsic mean, the $\log$ map is no more a bijection and centering the data is no longer possible with the presented methods. A solution to this problem would be, similarly to $\mathbb{R}^n$-based signals, to perform local covariance on a time segment short enough to consider the data localized enough. This can be explicitly written by adding a weight function into Equation 2 for windowing the time series.

Despite that Equation 4 is defined on $\mathcal{SO}(3)$, it can easily be generalized to any Lie group. It would also be possible to extend this method to Riemannian manifolds. Computing the mean can be done in a very similar manner and therefore, for a time series $X_t \in \mathcal{M}$, it can be mapped as a $T_{\bar{X}}\mathcal{M}$-based time series. The main issue comes from the translation, as it cannot be done by a simple multiplication. Given two time series, $X_t$ and $Y_t$, one needs to compare elements from $T_{\bar{X}}\mathcal{M}$ with elements from $T_{\bar{Y}}\mathcal{M}$. One way to do it would be to transport the elements from $T_{\bar{X}}\mathcal{M}$ from $\bar{X}$ to $\bar{Y}$ along a geodesic using parallel transport. Its reversibility ensures the symmetry of the method.

# 5 Conclusion

The definition of the covariance presented at Equation 4 gives a way to measure the synchronization between two $SO(3)$ based signals. This measure is useful for the study of body kinematics coordination for indoor climbing. A study applied to several climbers is in preparation to measure of effects of learning protocols on body coordination and skills.

It should be noted that this method works when the signals are localized around their means and that in other cases, the linearization might not be properly defined.

The definitions used here can easily be extended to any Lie groups and can be modified for processing Riemannian manifold based signals, using a parallel transport between the tangent spaces at the mean points.

# Références


[1] P. Cordier, M. Mendès France, P. Bolon, J. Pailhous. *Thermodynamic study of motor behaviour optimization*. Acta Biotheoretica, 42 : 187-201, 2015.

[2] L. Seifert, J Boulanger, D. Orth, K. David. *Environmental Design Shapes Perceptual-motor Exploration, Learning, and Transfer in Climbing*. Frontiers in Psychology, 2015.

[3] J. Boulanger, L.Seifert, R. Hérault, J-F. Coeurjolly. *Automatic Sensor-Based Detection and Classification of Climbing Activities*. IEEE Sensors, 2015.

[4] H. E. Cetingul, R. Vidal *Intrinsic mean shift for clustering on Stiefel and Grassmann manifolds* IEEE Conference on Computer Vision and Pattern Recognition, 2009.

[5] D. I. Nikolayev, T. I. Savyolov *Normal Distribution on the Rotation Group SO(3)* Textures and Microstructures, vol. 29, 1997

[6] R. Subbarao, P. Meer. *Nonlinear Mean Shift over Riemannian Manifolds*. International Journal of Computer Vision, 2009

[7] J. Boulanger. *Adaptive Filtering and Parametric Estimation for Random Processes on Rotation Groups and Stiefel Manifolds*. PhD Thesis, 2013.

[8] F. Baudoin, M. Hairer, J. Teichmann *Ornstein-Uhlenbeck processes on Lie groups*. Journal of Functional Analysis, 2008.

[9] J. Lee, S. Y. Shin *General construction of time domain filters for orientation data* IEEE Transactions on visualisation and computer graphics, vol. 8, pp. 119âĂŞ128, 2002.